J|A|C|S
ARTICLES
Published on Web 01/29/2002

Artificial Lamellar Mesostructures to WS_2 Nanotubes

Yadong D. Li,*[,†,‡] Xiaolin L. Li,[†] Rongrui R. He,[§] Jing Zhu,[§] and Zhaoxiang X. Deng[†]

Contribution from the Department of Chemistry, Key Laboratory of Atomic & Molecular Nanosciences (Ministry of Education, China), Department of Material Science & Engineering, and Tsinghua-Foxconn Nanotechnology Laboratory, Tsinghua University, Beijing 100084, People's Republic of China

Received August 28, 2001

Abstract: A direct pyrolysis method from artificial lamellar mesostructures to nanotubes was developed for the synthesis of tungsten disulfide (WS_2) nanotubes. In this process, a tungsten sulfide artificial lamellar mesostructure composite with intercalated cetyltrimethylammonium cations (WS-L) was prepared on the basis of the recently developed template self-assembly of anionic tungstates (WS_4^{2-}) and cationic surfactant molecules (CTA^+) in solution under appropriate conditions. After heating of this inorganic−surfactant lamellar composite material in an argon atmosphere to 850 °C, bulk quantities of uniform WS_2 nanotubes with diameters of 5−37.5 nm and lengths ranging from 0.2 to 5 μm were produced, which revealed a general rolling mechanism of layered sheets for tubule formation. The observations of transmission electron microscopy are in good agreement with the proposed rolling mechanism.

The discovery of carbon nanotubes in 1991[1] has initiated intense experimental and theoretical interest in such tubular structures. Over the past few decades considerable efforts have been placed on the synthesis of different kinds of nanotubes. A particularly significant breakthrough in WS_2 and MoS_2 nanotube synthesis was made by Tenne and co-workers[2] through the gas-phase reaction between MoO_3 or WO_{3-x} and H_2S in a reducing atmosphere at elevated temperature (800−1000 °C). Then, many other kinds of nanotubes such as BN nanotubes, BCN nanotubes,[3] $NiCl_2$ nanotubes,[4] vanadium oxide nanotubes,[5] TiO_2 nanotubes,[6] InS nanotubes,[7] NbS_2 nanotubes, TaS_2 nanotubes,[8] and organic nanotubes[9] through various approaches with different growth mechanisms have also been reported. Although all of the synthesized nanotube materials commonly possess sheetlike structural features, until now, no generalized synthetic method for nanotubes has been established for lack of suitable growth mechanisms. As is well-known, there are great amounts of naturally or artificially synthesized materials possessing

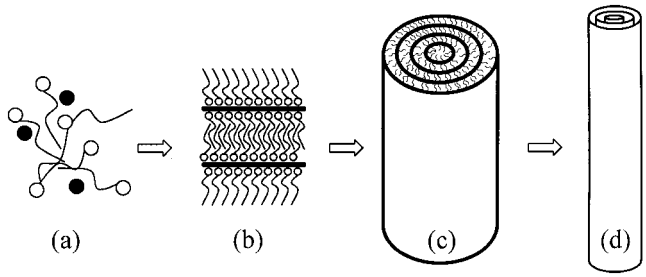

Figure 1. Schematic presentation of the whole rolling mechanism for the formation of WS_2 nanotubes: (a) homogeneous solution of CTA^+ and WS_4^{2-}, (b) assembly of CTA^+ and WS_4^{2-} into a lamellar structure, (c) rolling of lamellar inorganic−surfactant mesostructures into columnar structures, (d) removal of surfactant molecules and reduction of WS_4^{2-} to form WS_2 nanotubes under VPC conditions.

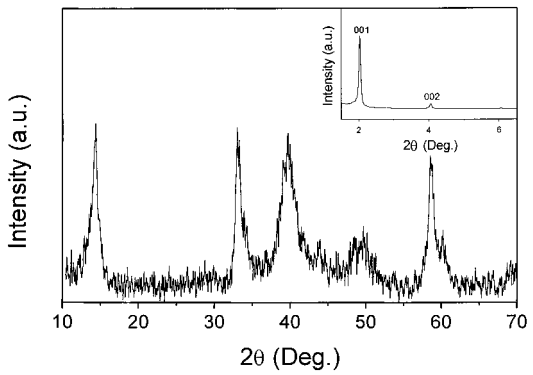

Figure 2. XRD patterns of the as-synthesized WS_2 products obtained after VPC processing of the precursors. The inset shows a low-angle XRD pattern of the inorganic−surfactant lamellar precursors. All the XRD results were recorded on a Bruker D8-Advance X-ray diffractometer with monochromatized Cu Kα incident radiation, recorded with a 2θ resolution of 0.02° and a scan rate of 0.5 s per point. The operation voltage and current are 40 kV and 40 mA, respectively.

[†] Department of Chemistry, Key Laboratory of Atomic & Molecular Nanosciences.
[‡] Tsinghua-Foxconn Nanotechnology Laboratory.
[§] Department of Material Science & Engineering.

(1) Iijima, S. *Nature* **1991**, *354*, 56.
(2) (a) Tenne, R.; Margulis, L.; Genut, M.; Hodes, G. *Nature* **1992**, *360*, 444. (b) Margwlis, L.; Salltra, G.; Tenne, R.; Talianker, M. *Nature* **1993**, 365, 144. (c) Feldman, Y.; Wasserman, E.; Srolovita, D. J.; Tenne, R. *Science* **1995**, *267*, 222.
(3) Chopra, N. G.; Luyren, R. J.; Cherry, K.; Crespi, V. H.; Cohen, M. L.; Louis, S. G.; Zettl, A. *Science* **1995**, 269−966.
(4) Hachohen, Y. R.; Grunbaum, E.; Sloan, J.; Hutchison, J. L.; Tenne, R. *Nature* **1998**, *395*, 336.
(5) (a) Spahr, M. E.; Betterli, P.; Nesper, R.; Miiller, M.; Krumeich, F.; Nissen, H. U. *Angew. Chem., Int. Ed.* **1998**, *37* (9), 1263. (b) Krumeich, F.; Muhr, H. J.; Niederberger, M.; Bieri, F.; Schnyder, B.; Nesper, R. *J. Am. Chem. Soc.* **1999**, *121*, 8324. (c) Niederberger, M.; Muhr, H. J.; Krumeich, F.; Bieri, F.; Gunther, D.; Nesper, R. *Chem. Mater.* **2000**, *12*, 1995.
(6) (a). Kasuga, T.; Hiramatsu, M.; Hoson, A.; Sekino, T.; Niihara, K. *Langmuir* **1998**, *14*, 3160. (b) Kasuga, T.; Hiramatsu, M.; Hoson, A.; Sekino, T.; Niihara, K. *Adv. Mater.* **1999**, *11*, 1307.
(7) Hollingsworth, J. A.; Poojary, D. M.; Clearfied, A.; Buhro, W. E. *J. Am. Chem. Soc.* **2000**, *122*, 3562.
(8) Nath, M.; Rao, C. N. R. *J. Am. Chem. Soc.* **2001**, *123*, 4841.
(9) (a) Ghadirl, M. R.; Granja, J. R.; Milligan, R. A.; McRee, D. E.; Khazanovich, N. *Nature* **1993**, *366*, 324. (b) Ghadirl, M. R.; Granja, J. R.; Buehler, L. K. *Nature* **1994**, *369*, 301.

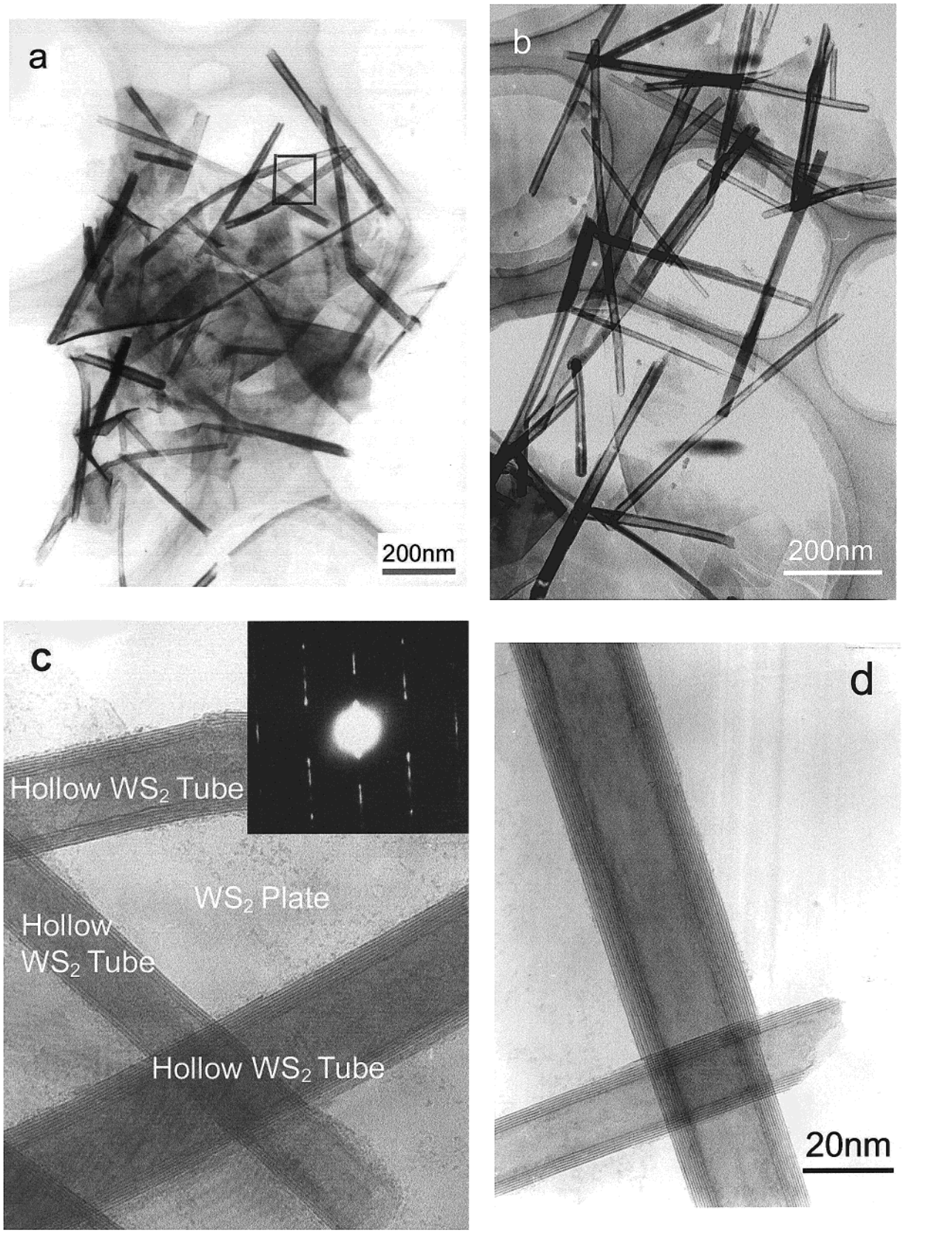

Figure 3. TEM images of the as-synthesized WS_2 nanotubes: (a, b) low-magnification TEM image and (c, d) high-resolution TEM image taken on a JEOL-2010 transmission electron microscope. The area indicated in (a) clearly shows the coexistence of hollow WS_2 nanotubes and WS_2 plates. The inset in (c) is a SEAD pattern taken on an individual nanotube.

layered (or sheetlike) structures, such as layered asbestos, chrysotil, brucite minerals,[10] lamellar solid acids, α-$Zr(HPO_4)_2 \cdot H_2O$, $HTiNbO_5$,[11] $K_4Nb_6O_{17}$, $K_2Ti_4O_9$,[12] $Bi_4Ti_3O_{12}$,[13] Bi_2Te_3, $CsBi_4Te_6$, $Cs_2Bi_4Se_7$, $Cs_3Bi_7Se_{12}$,[14] P, As, Sb, Bi,[15] and artifi-

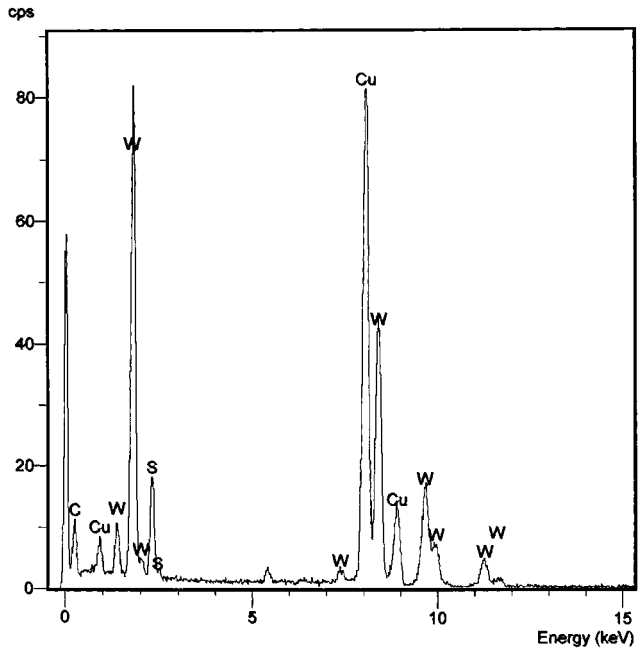

Figure 4. EDX analysis of the as-synthesized WS_2 nanotube. Cu peaks raised from the TEM grid.

cially synthesized inorganic−surfactant lamellar mesostructured materials.[16] Other layered compounds such as GaSe, NbS_2, and black phosphorus[17] have been the subjects of extensive theoretical investigations, which have predicted conditions for their stabilities in cylindrical form and some interesting electronic properties. Recently, we have developed a low-temperature hydrothermal reduction method and successfully synthesized Bi nanotubes.[18] Can we develop a general synthetic method to prepare these nanotubes from the above-mentioned sheetlike structural materials?

Natural phenomena give us many inspirations; a piece of foliage or a piece of wet paper curls naturally during its drying process. If appropriate actions are applied, they will often form tubular structures. On the basis of a similar principle, for a layered compound, if the interaction between neighboring layers could be reduced from the edges of the layer, while keeping the interactions of in-layer atoms or molecules, tubular structures (or nanotubes) might also form through the rolling of these lamellar structures.

The artificial lamellar structures we plan to employ for the synthesis of WS_2 nanotubes are inorganic−surfactant lamellar intercalates based on a co-condensation mechanism of anionic inorganic species with cationic surfactant molecules.[16] The inorganic species is WS_4^{2-}, and the surfactant we choose to form layered micelles is CTAB. If, under certain conditions, the interlayer interaction of this kind of lamellar intercalate could be diminished from the edges, rolling of the layers into tubules should be expected. Transformation of these tubules into WS_2 nanotubes could be realized through removal of the organic surfactants and reduction of WS_4^{2-} to WS_2. The above scheme for the formation of nanotubes is called the rolling mechanism, which could be divided into four steps: (i) The CTAB surfactant molecules condensed into aggregations with WS_4^{2-} anions intercalated into the interspaces between the headgroups of CTAB to form CTA−WS_4 ion pairs. (ii) The condensation process continued and brought out more ordered lamellar assemblies. (iii) When heated in a vacuum at gradually elevated temperature, these lamellar sheets began to loosen at the sheet edge and then rolled into separate scrolls, which were a combination of CTA cations and WS_4^{2-} anions. (iv) With increasing furnace temperature, in situ reduction of WS_4^{2-} by the pyrolyzed carbon from CATB happened and thus produced WS_2 with a morphology confined by the scrolls, which might serve as microreactors in the vacuum-pyrolysis-carbothermal (VPC) process and were responsible for the ultimate formation of tubular WS_2. The above process is schematized in Figure 1, and the whole reaction for the formation of WS_2 nanotubes can

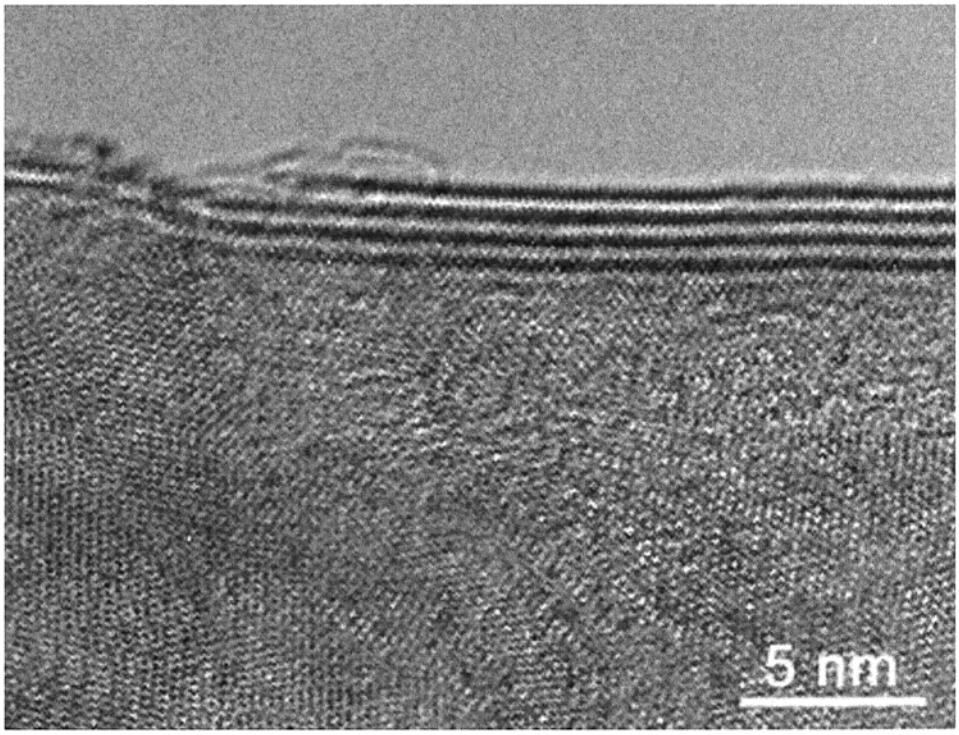

Figure 5. A HRTEM picture showing the curling at the edge of a WS_2 plate.

be expressed as

$$WO_4^{2-} + S^{2-} \xrightarrow{CTAB} (CTA^+)_2WS_4^{2-} \xrightarrow{VPC} WS_2$$

Mesolamellar tungsten sulfide (referred to as WS-L) with intercalated cetyltrimethylammonium (CTA^+) cations was prepared on the basis of a co-condensation mechanism of anionic inorganic species with a cationic surfactant (S^+I^-) under a mild hydrothermal condition.[16] Analytical grade sodium tungstate (Na_2WO_4; 3 mmol), CH_3CSNH_2 (9 mmol of thioacetamide), and cetyltrimethylammonium bromide (CTAB; 9 mmol) were dissolved in distilled water to form a homogeneous solution. The pH of the solution was adjusted to the range of 8−10 by addition of aqueous NH_3 or HCl. The mixture was stirred vigorously for 1 h and then sealed in a Teflon-lined stainless steel autoclave and kept at 140 °C for 6 days. The solid WS-L products were filtered, washed with distilled water and absolute ethanol, and then dried in a vacuum at 80 °C for 12 h. The calculated yield was about 85−90% on the basis of W. The chemical analysis and TG/DTA results showed a molar ratio of surfactant to tungsten of 2:1. The typical lamellar feature of WS-L was confirmed by the low-angle X-ray powder diffraction pattern (inset of Figure 2).

The VPC synthesis of the inorganic−surfactant lamellar (WS-L) precursor was carried out in a conventional tube furnace. The as-prepared WS-L precursor was placed in a quartz boat. The quartz boat was placed in the hot zone inside the quartz tube and then calcined and pyrolyzed for 12 h at elevated temperature from 100 to 850 °C in a high-purity argon atmosphere (99.999%) with a pressure range of 10^{-2} to 10^{-3} atm. The reaction temperature was controlled exactly at ±1 °C by a built-in temperature control unit in the tube furnace. Control of the temperature gradient and gas pressure in the course of the VPC reaction is a key factor; otherwise, the precursors will be cracked into platelets or particles.

(10) (a) Bates, T. F.; Sand, L. B.; Mink, J. F. *Science* **1950**, *111*, 512. (b) Yada, K. *Acta Crystallogr.* **1967**, *23*, 704. (c) Frazier, S. E.; Bedford, J. A.; Hower, J.; Kenney, M. E. *Inorg. Chem.* **1967**, *6*, 1693.

(11) (a) Kaschak, D. M.; Johnson, S. A.; Hooks, D. E.; Kim, H.; Ward, M. D.; Mallouk, T. E. *J. Am. Chem. Soc.* **1998**, *120*, 10887. (b) Kerimo, J.; Adams, D. M.; Barbara, P. F.; Kaschak, D. M.; Mallouk, T. E. *J. Phys. Chem. B* **1998**, *102*, 9451. (c) Kim, H.; Keller, S. W.; Mallouk, T. E.; Schmitt, J.; Decher, G. *Chem. Mater.* **1997**, *9*, 1414. (d) Fang, M.; Kim, H. N.; Saupe, G. B.; Miwa, T.; Fujishima, A.; Mallouk, T. E. *Chem. Mater.* **1999**, *11*, 1526.

(12) (a) Nassau, K.; Shiever, J. W.; Bernstein, J. L. *J. Electrochem. Soc.* **1969**, *116*, 348. (b) Lagaly, G.; Beneke, K. *J. Inorg. Nucl. Chem.* **1976**, *38* (8), 1513. (c) Kinomura, N.; Kumada, W.; Muto F. *J. Chem. Soc., Dalton Trans.* **1985**, *11*, 2349. (d). Dion, M.; et al. *J. Inorg. Nucl. Chem.* **1978**, *40*, 917.

(13) (a) Bersukova, M. L.; et al. *J. Cryst. Growth* **1972**, *13/14*, 503. (b) Bruton, T. M. *Ferroelectrics* **1974**, *7*, 259. (c) Subbarao, E. C. *J. Am. Ceram. Soc.* **1962**, *45*, 166.

(14) (a) Iordanidis, L.; Kanatzidis, M. G. *Angew. Chem., Int. Ed.* **2000**, *112*, 2004. (b) Iordanidis, L.; Kanatzidis, M. G. *J. Am. Chem. Soc.* **2000**, *122*, 8319. (c) Chung, D. Y.; Hogan, T.; Brazis, P.; Rocci-Lane, M.; Kannewurf, C.; Bastea, M.; Uher, C.; Kanatzidis, M. G. *Science* **2000**, *287*, 1024.

(15) Wyckoff, R. W. G. *Crystal structures*, 2nd ed.; Interscience: New York, 1963; Vol. 1, pp 30−32.

(16) (a) Alfredssoon, V.; Keung, M.; Monnier, A.; Stucky, G. D.; Unger, K. K.; Schuth, F. *J. Chem. Soc., Chem. Commun.* **1994**, 921−922. (b) Yang, P. D.; Zhao, D. Y.; Margolese, D. I.; Chmelka, B. F.; Stucky, G. D. *Nature* **1998**, *396*, 152−155. (c) Yang, P. D.; Zhao, D. Y.; Margolese, D. I.; Chmelka, B. F.; Stucky, G. D. *Chem. Mater.* **1999**, *11*, 2813. (d) Wang, Y.; Chen, J. S.; Yu, S. F.; Xu, R. R. *Chem. J. Chin. Univ.* **2000**, *21* (2), 165. (e) Huo, Q. S.; Margolese, D. I.; Ciesla, U.; Feng, P. Y.; Gier, T. E.; Sieger, P.; Leon, R.; Petroff, P. M.; Schuth, F.; Stucky, G. D. *Nature* **1994**, *368*, 317.

(17) (a) Côté, M.; Cohen, M. L.; Chadi, D. J. *Phys. Rev. B* **1988**, *58*, R4277. (b) Seifert, G.; Terrones, H.; Terrones, M.; Frauenheim, T. *Solid State Commun.* **2000**, *115*, 635. (c) Seifert, G.; Hernandez, E. *Chem. Phys. Lett.* **2000**, *318*, 355.

(18) Li, Y. D.; Wang, J. W.; Deng Z. X. Wu, Y. Y.; Sun, X. M.; Yu, D. P.; Yang P. D. *J. Am. Chem. Soc.* **2001**, *123*, 9904.

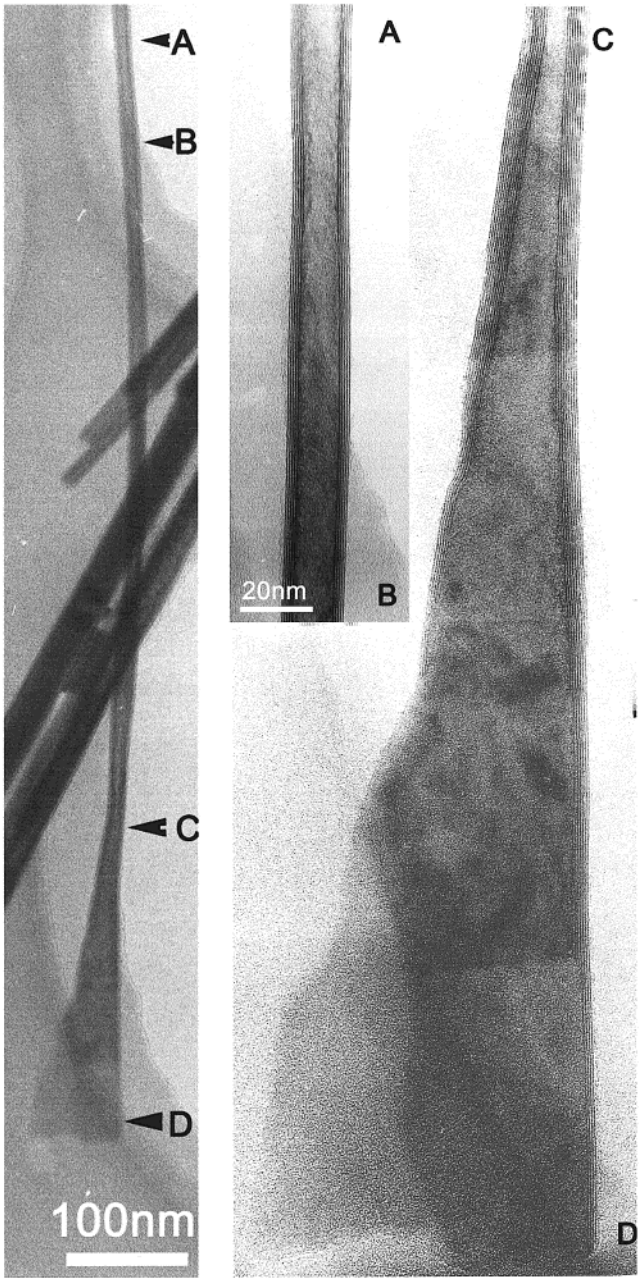

Figure 6. TEM image of a half-tube and half-plate structure. D → C → B → A shows the transition from a platelike structure to a tubular structure.

The XRD pattern in the 2θ range of 10−70° of the black product after heat treatment is shown in Figure 2. Despite the broadened peaks, the XRD pattern could be indexed by the 2H (hexagonal) polymorph of WS_2 (JCPDS card 84-1398). The TEM image of a typical product (Figure 3a,b) obtained through the above VPC method is characteristic of high-quality tubular structures with outer diameters of 15−30 nm and lengths ranging from hundreds of nanometers to several micrometers. High-resolution transmission electron microscopy (HREM) images of products (Figure 3c,d) unambiguously reveal that the obtained tubular structures are exclusively multiwalled nanotubes. Different from the WS_2 nanotubes obtained through surface sulfuration of needlelike WO_3, there are no encapsulated WO_3 particles in these nanotubes, which might suggest a different formation mechanism of these hollow WS_2 nanotubes. The selected area electron diffraction (SAED) pattern (inset in Figure

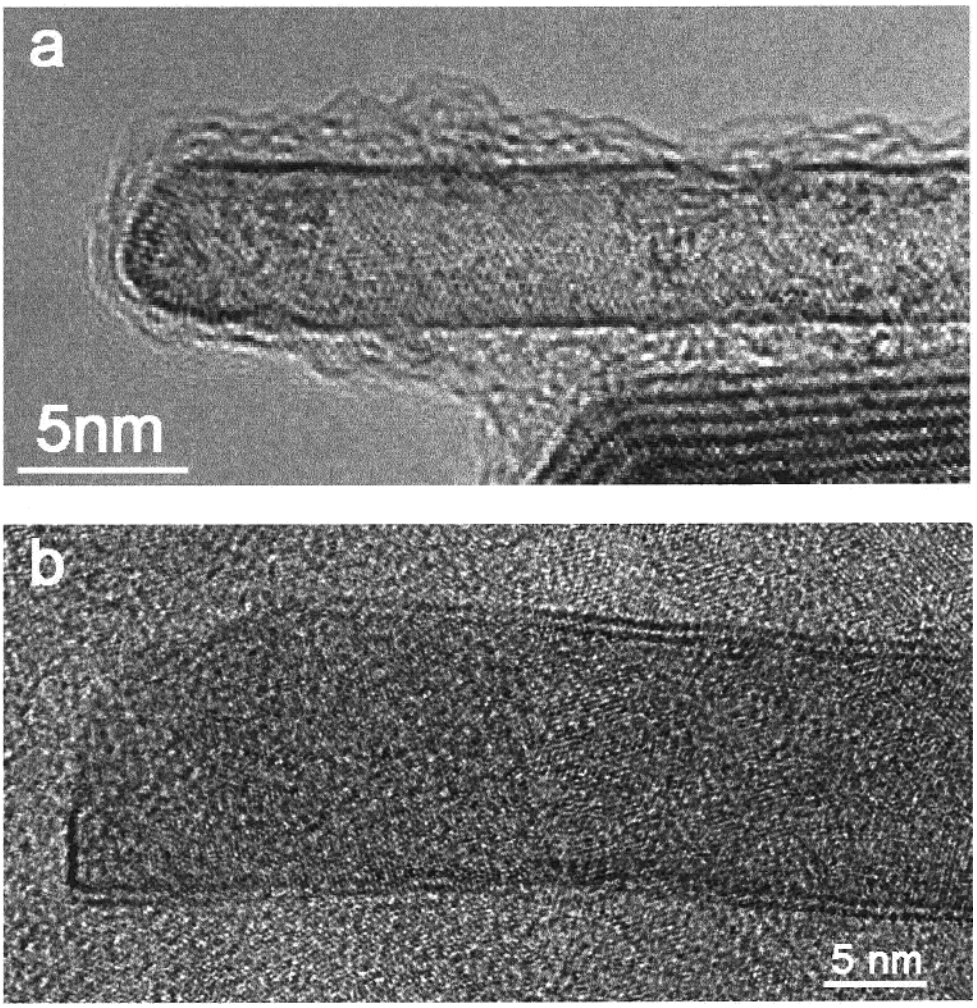

Figure 7. HRTEM image of single-walled (a) and double-walled (b) hollow WS_2 nanotubes.

3c) recorded for a single nanotube shows reflections characteristic of the planes perpendicular to the electron beam. Diffuse diffraction spots in the SAED pattern are due to the cylindrical structure of the sample. On the basis of the 002 diffraction spots corresponding to the planes parallel to the electron beam, a spacing of 6.2 Å, equal to half the *c*-axis constant of WS_2, could be derived. This value was also in agreement with the lattice fringes shown in Figure 3 c,d. Energy-dispersive X-ray analysis (EDX) (Figure 4) taken on individual nanotubes exhibited the existence of W and S with a molar ratio close to 1:2.

In the case of the chirality of the as-synthesized nanotubes, we have observed different helical angels in multishelled nanotubes. Sometimes all the layers in a nanotube show only one helicity, such as the ED pattern shown in Figure 3, which shows a tube axis of 110 corresponding to a chiral angle of 30°. But we have also observed different helicities in one multiwalled WS_2 nanotube. So the synthetic approach we have reported did not show control of the helicity of the products.

Extensive and careful HRTEM observations confirmed the rolling mechanism. First, there is a notable characteristic for the distribution of the product; that is, the WS_2 nanotubes always coexist with large WS_2 plates, as illustrated in Figure 3c. This suggests the link between the WS_2 nanotubes and the WS_2 plates and corresponds with the rolling mechanism well. WS_2 plates with a relatively large size were more difficult to roll than those with a small size, hence the unrolled plates left with WS_2 nanotubes after small plates finished rolling. Second, many WS_2 plates with curled edges were often found. Figure 5 is a typical example. These plates can be considered as being in the initial stage of rolling. Third, there is more direct evidence for the rolling mechanism found in a half-tube and half-plate structure, as shown in Figure 6. This HRTEM image clearly indicates the coexistence of tubes and sheets in the same structure. In the zone indicated by letter A, a perfect tubular structure with a diameter of 20 nm has already been formed, while in the zone marked by D, rolling only happened at the edge of the sheet, and in zone C transition from a tubular to sheetlike structure can be found. These completely and incompletely formed tubular structures are believed to be left during the rolling process of the lamellar inorganic−surfactant under VPC processing. Finally, single-walled and double-walled hollow WS_2 nanotubes found in the product provide additional evidence for the rolling mechanism. Figure 7a shows a single-walled WS_2 nanotube with a diameter of 5 nm, and Figure 7b shows a double-walled WS_2 nanotube with a diameter of 14 nm. These hollow WS_2 nanotubes with a rather large diameter could not be formed through other processes such as surface sulfuration of needlelike tungsten oxide because it is hard to imagine that the inner core could be consumed completely in a WO_{3-x} nanowire, leaving just a very thin shell.

This novel rolling mechanism for the formation of nanotubes from a lamellar structure requires a clear understanding.

Heidenreich et al.[19] have noted that severe bending of graphite sheets commonly occurs at high temperature. More recently, curling of graphitic networks has been observed under electron beam irradiation.[20] This suggests that a high temperature or thermal stress may initiate bending of layered structures. These findings further strengthen the possibility of the rolling process of the lamellar inorganic−surfactant mesostructures we suggested for the formation of tubular structures. Thus, the driving force for the curling of the lamellar sheets could be ascribed to (1) the reduction of interlayer interaction at the edge of the sheet during the heating process and (2) the thermal stress existing at high temperature, which initiates the scrolling of the layered sheets with reduced interlayer forces at the edges.

Our experiment results are in good agreement with the predictions of our model, which suggests that it should be possible to rationally choose proper growth conditions for nanotube synthesis from other lamellar layer structures including natural or artificial lamellar structures. To conduct a stringent test of our proposed rolling mechanism, very recently we have chosen layered $H_2Ti_4O_9$ for preparing $H_2Ti_4O_9$ nanotubes. Successful synthesis of $H_2Ti_4O_9$ nanotubes and its metal-substituted derivatives, MTi_4O_9 nanotubes,[21] provides strong support for the generality of our approach. In fact, one of our former experimental results on the synthesis of bismuth nanotubes has given us strong inspiration. The formation mechanism of the Bi nanotubes should be associated with the rolling from its pseudolayered structure. It is also noteworthy that, in the earlier work of Domen and Mallouk[22,23] on the chemical transformation of lamellar oxides into single-sheet colloids, tubular structures, and unilamellar sheets, the rolling phenomenon was also observed and interpreted, which also revealed the possibility for a lamellar sheet to form a tubular structure through a similar rolling process. On the basis of our research, we believe that it would be possible to prepare other novel nanotube materials with various electrical, magnetic, optical, and optoelectric properties from a natural or artificial lamellar structure under proper experimental conditions.

Acknowledgment. We thank Prof. S. S. Fan for helpful discussions. This work was supported by NSFC through the National Outstanding Youth Science Fund (Y.L.) (Grant No. 20025102) and the State Key Project of Fundamental Research for Nanomaterials and Nanostructures (Grant No. G19990645-03).

JA012055M

(19) Heidenreich, R. D.; Hess, W. M.; Ban, L. L. *J. Appl. Crystallogr*. **1968**, *1*, 1.
(20) Ugarte, D. *Nature* **1992**, *359*, 707.
(21) Li, Y. D.; Sun, X. M.; Deng, Z. X.; et al. $H_2Ti_4O_9$ nanotube and its metal substituted derivatives MTi_4O_9 nanotubes. Unpublished results.
(22) (a) Abe, R.; Shinohara, K.; Tanaka, A.; Hara, M.; Kondo, J.; Domen, K. *J. Mater. Res.* **1998**, *13*, 861. (b) Abe, R.; Shinohara, K.; Tanaka, A.; Hara, M.; Kondo, J.; Domen, K. *Chem. Mater.* **1997**, *9*, 2179.
(23) (a) Saupe, G. B.; Waraksa, C. C.; Kin, H. N.; Han, Y. J.; Kaschak, D. M.; Skinner, D. M.; Mallouk, T. E. *Chem. Mater.* **2000**, *12*, 1556. (b) Schaak, R. E.; Mallouk, T. E. *Chem. Mater.* **2000**, *12*, 3427.